Tethys
Journal of Mediterranean Meteorology & Climatology

Tethys 2014, **11**, 13–23
www.tethys.cat
ISSN-1697-1523
eISSN-1139-3394
DOI:10.3369/tethys.2014.11.02
Journal edited by **ACAM**

Synoptic and mesoscalar environments associated with the heavy local rainfall on 16 August 2010 in the south of the Iberian Peninsula

J. M. Sánchez-Laulhé, J. Riesco, F. Polvorinos and J. D. Soriano

Agencia Estatal de Meteorología, C/ Demostenes, 4, 29010, Málaga

Received: 11-XII-2012 – Accepted: 21-I-2014 – **Original version**

Correspondence to: jsanchezlaulheo@aemet.es

Abstract

In this paper we show the synoptic and mesoscale environment aspects associated with a local event of heavy rainfall in the south of the Iberian Peninsula on 16 August 2010, exceeding 200 mm in 5 hours and causing significant flash flooding, by using observational data and operational analyses and forecast data from the European Centre for Medium-Range Weather Forecasts. The event was associated with the poleward transport of deep tropical moisture along the western flank of the upper and middle level summer anticyclone over North Africa, and with a mid-level cyclogenesis caused by the interaction between a middle latitude trough and the tropical moisture band. The cyclogenesis produced an outflow jet streak and the exportation of tropical moisture to the Iberian Peninsula. On the synoptic scale, the heavy precipitation occurred where this tropical moisture intersected a region of forced ascent situated beneath the equatorward jet streak-entrance region. On the mesoscale, the event was focused on a zone of orographic wind convergence.

Key words: Flash flood, Iberian Peninsula, elevated convection, tropical-extratropical interaction, dry line, mid-level cyclogenesis

1 Introduction

This is a meteorological analysis of the deadly flash flood that occurred in Andalusia, a region in the south of Spain, in the province of Córdoba during the night of 16-17 August 2010. It caused three fatalities: a man and a woman who were dragged downstream near Aguilar de la Frontera and another man who was killed when a wall collapsed in his home at Bujalance (Figure 1).

The distribution of heavy precipitation was highly localized. Only in two of the weather stations in the AEMET network, both of them in the municipality of Aguilar de la Frontera, did the precipitation accumulated on the 16th rise above 200 mm, and only in the three stations of Aguilar and one of Bujalance, did it rise above 100 mm. This distribution is confirmed by the rain accumulation product of the Seville radar (Figure 2). Accompanying the rainstorms, very strong wind gusts were registered (maximum of 71 km h^{-1} in Aguilar) and hail was also observed in several towns.

Figure 3 represents the precipitation in the automatic weather station of Laguna de Zoñar (in the municipality of Aguilar) at ten-minute intervals. The maximum values of accumulated precipitation were 23 mm in 10 minutes, 41 mm in 20 minutes, 60 mm in 30 minutes, 111.6 mm in one hour, 162.4 mm in two hours and 212.6 mm in less than twelve hours.

As a reference, the monthly average total precipitation for August in the manual station of Aguilar de la Frontera is 7.1 mm and in Cordoba-Airport (the reference station in the province), it is only 3 mm. Summer is critically dry in southern Spain (Font, 1983) as it is in other areas of the Mediterranean region as a result of its latitude (36-44°N), being a transition zone between the mid-latitude low pressures and the subtropical highs that impose strong seasonal contrasts.

The Spanish Mediterranean area is often affected by heavy convective rain, especially during autumn. Most observing stations in this area have maximum recorded rainfall amounts of over 200 mm in the autumn (Font, 1983).

Figure 1. Major terrain and geographic features of southern Iberian Peninsula with the situation of Aguilar de la Frontera and Bujalance.

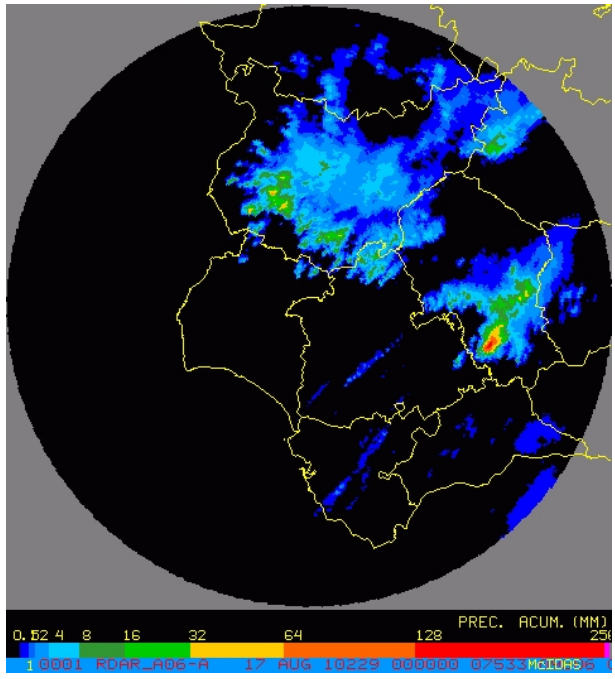

Figure 2. Accumulated precipitation in six hours, 18:00-24:00 UTC, on day 16, as seen by Seville radar. The value of this product in Aguilar was 144 mm.

Romero et al. (1999) derived the main spatial patterns presenting 'torrential' daily rainfalls in this area (torrential days as days with rainfalls exceeding 50 mm registered at 4 or more meteorological stations). They observed for torrential events, the dominant role exerted by the complex topography despite the large proportion of convective rainfalls; the greater frequency of cases in coastal zones; the higher frequency in autumn and winter for events largely stimulated by Atlantic flows and in the autumn season for those strongly influenced by the Mediterranean dynamics. Autumn is the most substantial season for all the area except for Andalusia, which tends to manifest lightly higher frequencies of torrential events in winter than in autumn. Along June, July and August, torrential events are oddly observed.

So, taking the preceding paragraphs into account, the value of the rainfall in one hour (111.6 mm between 21:00 and 22:00 UTC) during a summer evening, and in a location away from the coastline, must be considered exceptional and justifies the description of synoptic and mesoscale environmental aspects, which is the object of this paper.

Phenomenological and synoptic studies have been carried out on Spanish Mediterranean flood cases (e.g. García-Dana et al., 1982). These events are typically associated with the presence of a cold trough or a cut-off low located in the south-west of the Iberian Peninsula; these produce south-westerly diffluent flow in the middle and high troposphere over the western Mediterranean. At the lowest level, an easterly flow from the Mediterranean towards the Spanish coast provides warm, moist air to feed the convection.

The synoptic and mesoscale conditions in which heavy rain events occur in warm seasons are best documented in the USA (e.g., Maddox et al., 1979; Doswell III et al., 1996; Brooks and Stensrud, 2000; Schumacher and Johnson, 2005, 2006): Heavy rainfall events often occur beneath the equatorward jet-entrance region of an upper-level jet streak where broad quasi-geostrophic forcing for ascent can provide a favourable environment for deep-layer moisture and destabilization (e.g., Uccellini and Johnson, 1979; Bosart and Lackmann, 1995). Within this favourable synoptic-scale environment, mesoscale features such as baroclinic zones (e.g., Maddox et al., 1979; Junker et al., 1999; Moore et al., 2003; Schumacher and Johnson, 2005, 2006) and mountain barriers (e.g., Maddox et al., 1978; Caracena et al., 1979; Pontrelli et al., 1999) can act as focusing mechanisms for vigorous ascent.

The remainder of this paper is organized as follows. The large scale environment and the synoptic evolution are described in section 2. Mesoscale features associated with the event are presented in section 3. In section 4, an interpretation of the persistence of the rainfall in Aguilar is given. Finally, section 5 summarizes the key findings given in the paper and provides concluding remarks.

Throughout the study observational data have been used, and also outcome data from the global deterministic forecast and analysis model of the ECMWF (European Centre for Medium-Range Weather Forecasts) Integrated Forecast System (IFS) run in operational mode, that is to say, a spectral model based on a spherical harmonics expansion, with a spatial resolution T1279 (∼16 km grid spacing) and a vertical resolution of 91 levels (Simmons et al., 1989; Miller et al., 2010).

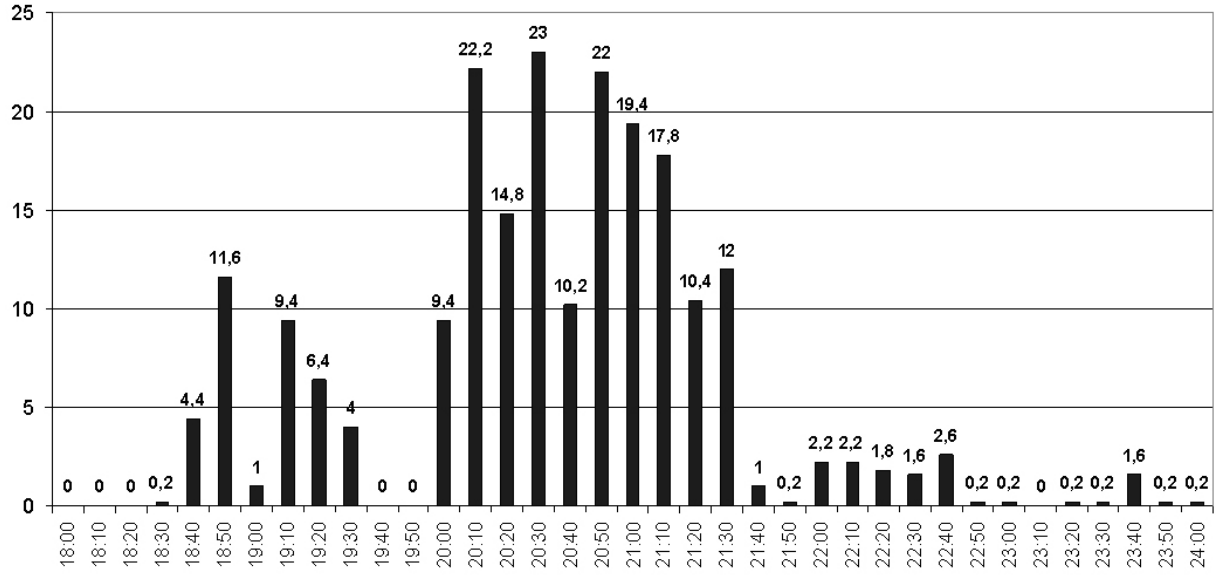

Figure 3. Rainfall (mm) registered in the automatic weather station of Laguna de Zoñar (Aguilar de la Frontera) at ten-minutes intervals (16 August 2010).

2 Synoptic and large scale environments

Upper and middle level maps of the previous day, August 15th, at 12:00 UTC, are shown in Figure 4. In Figure 4a, over a coloured water vapour (WV) 6.2 μm Meteosat Image, the fields of wind and geopotential height at 250 hPa show the next elements: a positive tilted trough poleward of the Canary Islands and east of the Azores, a ridge west of the Azores, and an anticyclone over North Africa. In Figure 4b, over an infrared (IR) 10.8 μ image, you can see the same elements and also an equatorial inverted trough can be observed at mid levels (500 hPa). The presence of a cold trough or a cut-off low in the upper and middle level over the southwest of the Iberian Peninsula is habitual in heavy rain events in Andalusia (Martinez et al., 2008). Along the northern stretching axis of the deformation pattern made up of by these troughs and highs (bold white lines in Figure 4b), deep moist continental tropical air and dry Atlantic air are exported northward, towards extra-tropical latitudes along the west coast of North Africa, forming an elongated tropical plume and a dry line at mid levels, as can be seen in the WV image (Figure 4a) and in the field of total precipitable water (TPW) column shown in Figure 4b. The dry air came from an upper level warm air pool, shown as the Atlantic reddish zone of the WV image (Figure 4a). The structure of the warm air pool is characterized by a strong potential temperature anomaly at upper levels (Figure 5), a deep warm anomaly extending throughout the column beneath the elevated tropopause and also by a negative anomaly of the potential vorticity (PV) in the upper layer of the troposphere.

The dry line can be characterized by the thermal front parameter (TFP), defined as:

$$TFP = -\nabla \left|\nabla\theta_e\right| \cdot \frac{\nabla\theta_e}{\left|\nabla\theta_e\right|} \quad (1)$$

where θ_e is the equivalent potential temperature.

Both, the increasing of TFP at 500 hPa (Figure 5) and the increasing of TPW (over 60 mm; not shown), at 00:00 UTC in the vicinity of the Canary Islands are indicative of frontogenesis and their associated vertical motions. The frontogenesis occurred when the baroclinic jet, associated to the forward side of the midlatitude trough, moved over the dry line, with the area of the frontogenesis located at the eastern entrance of the jet-streak (Figure 5b).

The frontogenesis was preceded by a weak mid-level cyclogenesis that had the effect of moistening the dry air strip existing between Africa and the Iberian Peninsula (Figure 4a), causing the consequent moistening of the air mass over the south part of Spain.

The process of mid-level cyclogenesis induced a folding of the tropopause, with the consequent descent of high PV tropopause air to the mid levels of the troposphere along a SW to NE elongated area located at 12:00 UTC over Morocco (Figure 6a), associated to the jet streak transversal vertical circulations. In Figure 6c and Figure 6d, on the coloured images of water vapour, the wind fields at 250 hPa and vertical velocity at 600 hPa, at 12:00 and 18:00 UTC are represented, and a clear correlation between the descending vertical velocity and mid-level PV positive anomaly at the 500-600 hPa layer (Figure 6e and Figure 6f) can be appreciated in the area with elongated descents. In the fields of relative humidity (RH) at 500 hPa of Figure 6e and Figure 6f, as

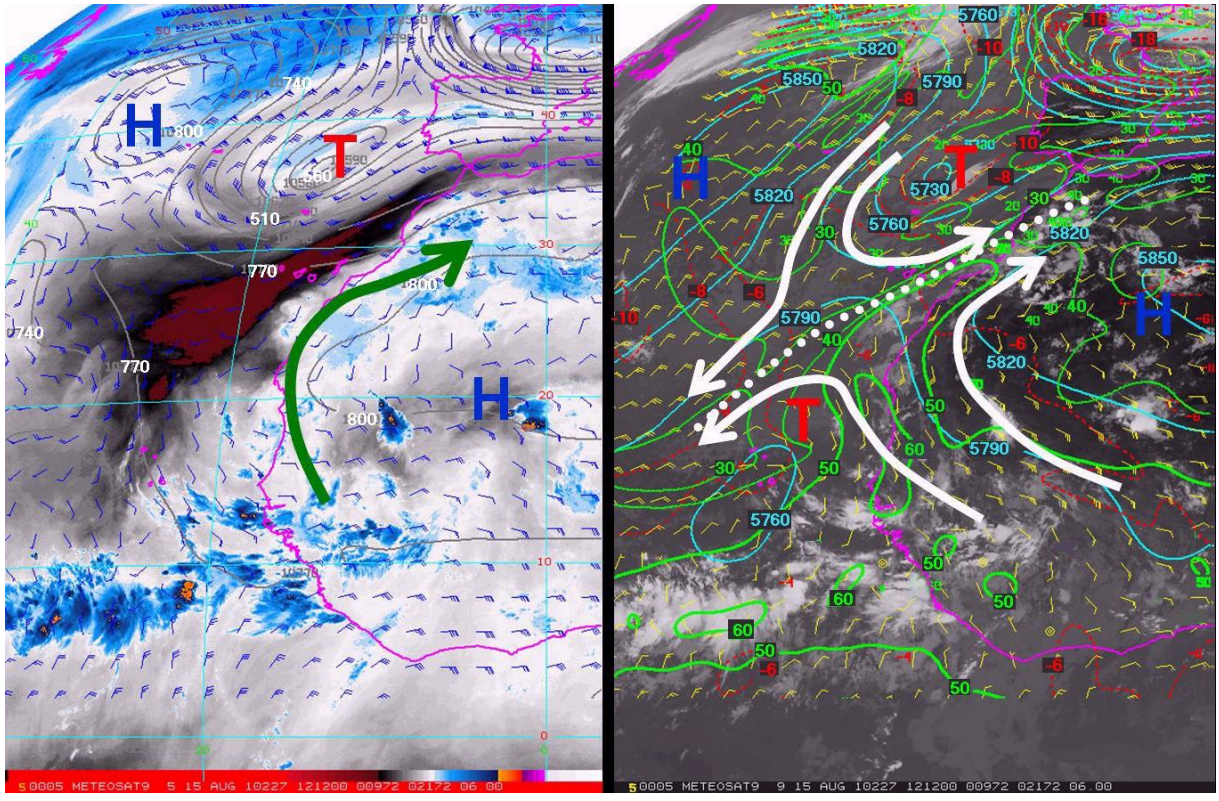

Figure 4. (a, left) 12:00 UTC 15 August Meteosat-9 WV 6.2 μm image; wind vectors (plotted as conventional wind barbs in knots) and geopotencial height (grey contours, interval 3 dam) at 250 hPa; (b, right) 12:00 UTC 15 August Meteosat-9 IR10.8 μm image; total column precipitable water (green contours, interval 10 mm) and geopotencial height (cyan, interval: 60 dam) and wind vectors at 500 hPa.

compensation for the isentropic descent of dry air in the folding of the tropopause, ascent of moist and saturated air, can be observed, mainly in the poleward extreme of the band of PV anomaly at midlevels (Figure 6d and Figure 6f), where the head of the comma-shaped cloud was formed. These dynamics are explained by the conceptual model about the structure of a cyclone during a coupling with a depression of the tropopause of Browning et al. (2000), but with the cyclogenesis occurring at mid-levels rather than at lower levels. In this model two rather symmetrical flows interwinning around a cyclone center: a dry-intrusion flow descending from the mesoscale tropopause depression and a flow of high-wet bulb potential temperature air ascending into the cloud head. An upper-level jet streak occurs at the leading edge of the mesoscale tropopause depression and the outflow from the cloud head feeds an upper-level outflow jet. The ascent of the high-wet bulb potential temperature flow is responsible for the upper parts of a cloud head, whose top rises toward a characteristically curved convex outer boundary. The area of descending dry-intrusion air extends down from the region of the tropopause depression. The stratospheric part of the dry intrusion descends beneath a jet streak as a tropopause fold into the middle and lower troposphere. Nearby tropospheric air also descends and gives rise to an extension of the dry intrusion.

In addition to deep-layer moistening, the cyclogenesis caused thermal destabilization in the south of the Iberian Peninsula, as can be seen in Figure 7, where the Lifted Index 700 (LI700: temperature difference between an air parcel lifted adiabatically from the surface to 700 hPa and the temperature of the environment at this pressure level) field at 18:00 UTC on the 16th is shown. Also the cyclogenesis caused the building up of an outflow anticyclonic upper level jet, that is also shown in Figure 7, whose equatorward jet-entrance region was located above the province of Cordoba at that time, something that is similar to that frequently found in warm season heavy rain events in the USA.

The synoptic environment of this event, with the presence of tropical moisture, had similitude with that of predecessor rainfall events (PREs). PREs, first defined by Cote (2007), are coherent mesoscale regions of heavy rainfall, exceeding 100 mm in 24 hr, that can occur approximately 1000 km poleward of recurving tropical cyclones (TCs) over the eastern third of the United States, associated with the poleward transport of deep tropical moisture ahead of the recurving TC, and located where this deep tropical moisture intersects a region of forced ascent above and north of a low-level baroclinic zone beneath an equatorward jet-entrance region (Cote, 2007 and Galarneau et al., 2010). In the case of the Aguilar location, the heavy rain occurred also beneath an

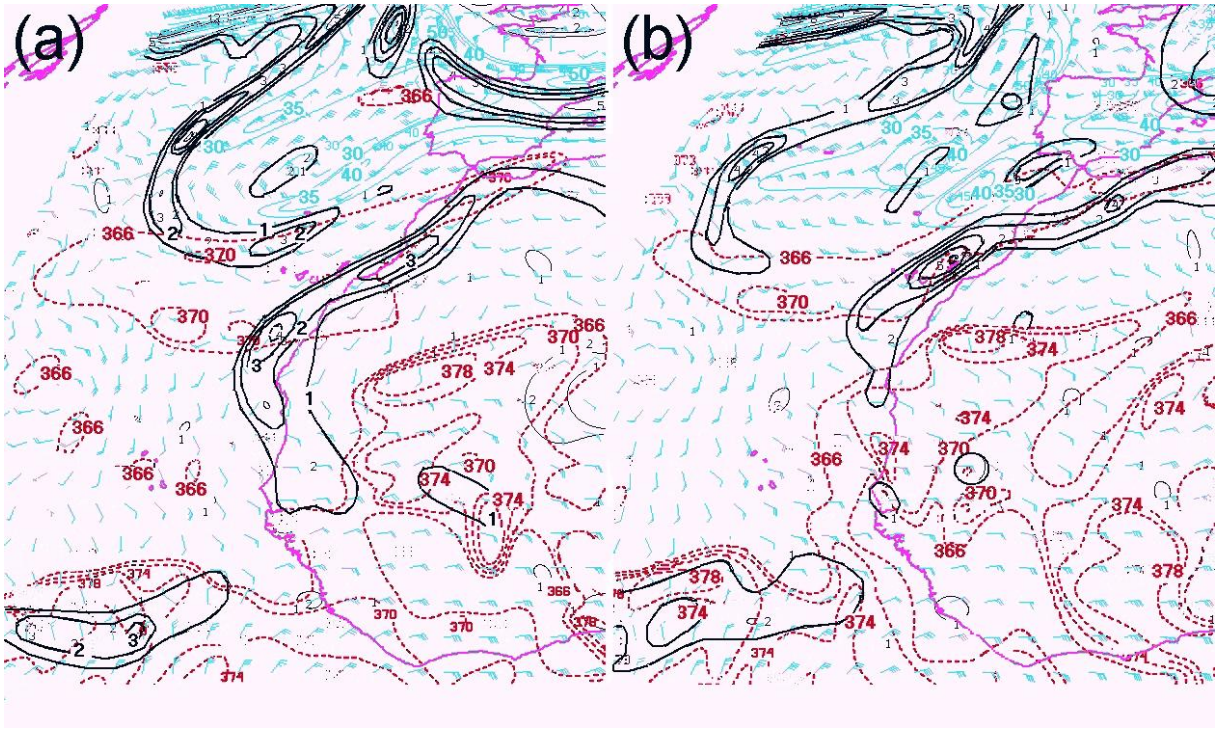

Figure 5. Wind vectors (plotted as conventional wind barbs in knots), isotachs (blue, interval: 5 m s^{-1}, beginning at 30 m s^{-1}), and potential temperature (dashed red contours beginning at 366 K; interval: 4 K) at tropopause, and thermal frontal parameter (solid black contours; interval 1 K m^{-2}) at 500 hPa (a) 12:00 UTC 15 August, and (b) 00:00 UTC 16 August.

equatorward jet entrance region, and a poleward transport of tropical moisture was present too, but differently the tropical moisture was transported poleward directly from the convection of the African monsoon over West Africa.

3 Mesoscale aspects

In this section, we try to examine the mesoscale features that could act as focusing mechanisms for the vigorous ascents, within the favourable synoptic-scale environment. In other heavy rain events, these mesoscale features have turned out to be baroclinic zones (e.g., Maddox et al., 1979; Glass et al., 1995; Junker et al., 1999; Moore et al., 2003; Schumacher and Johnson, 2005, 2006) and mountain barriers (e.g., Maddox et al., 1978; Caracena et al., 1979; Pontrelli et al., 1999). In both circumstances, a low-level jet was important in advecting warm, moist air into the region of heavy precipitation. Furthermore, a low-level jet oriented perpendicular to a surface boundary can result in enhanced low-level warm advection and moisture convergence and vigorous ascent (e.g., Maddox et al., 1979; Augustine and Caracena, 1994; Trier et al., 1996).

3.1 Convective bands

At 18:00 UTC on August 16, the area southward of the maximum wind and eastward of the upper level positive anomalies of PV, associated with the mid-latitude trough, was very cloudy, with low values of PV in the 250-300 hPa layer (mostly in the range 0.0 to 0.2 PVU, potential vorticity units) (Figure 8-9a). The colder cloud top areas (coloured) of IR Meteosat image showed a high correlation with convection areas with values of PV very close to zero, which are highlighted in grey in Figure 8. One of these areas is the elongated one LL', plotted as a bold dashed line, which corresponds to the convective cloud lineal band in the satellite image, marked also with LL' in Figure 9a.

The convective band formed within the ascending branch of a secondary circulation, associated with the direct vertical circulation of the entrance zone of a jet stream maximum aloft. The band occurred downstream of complex terrain of the western Betica Range, near the Strait of Gibraltar, on the anticyclonic shear side of the jet stream, where conditional, and possibly both dry symmetric (negative PV), and inertial (negative absolute vorticity) instabilities were present. The implication of the convection line LL' in the event seems quite evident when the sequence of IR images of the event are observed (Figure 9). Heavy rainfall ceased when the band finished crossing the area.

Through simulations using a convection-permitting numerical model Schumacher et al. (2010) studied the mechanisms responsible for the development and organization of bands of convection observed in events in the western United States on the anticyclonic shear side of strong mid-

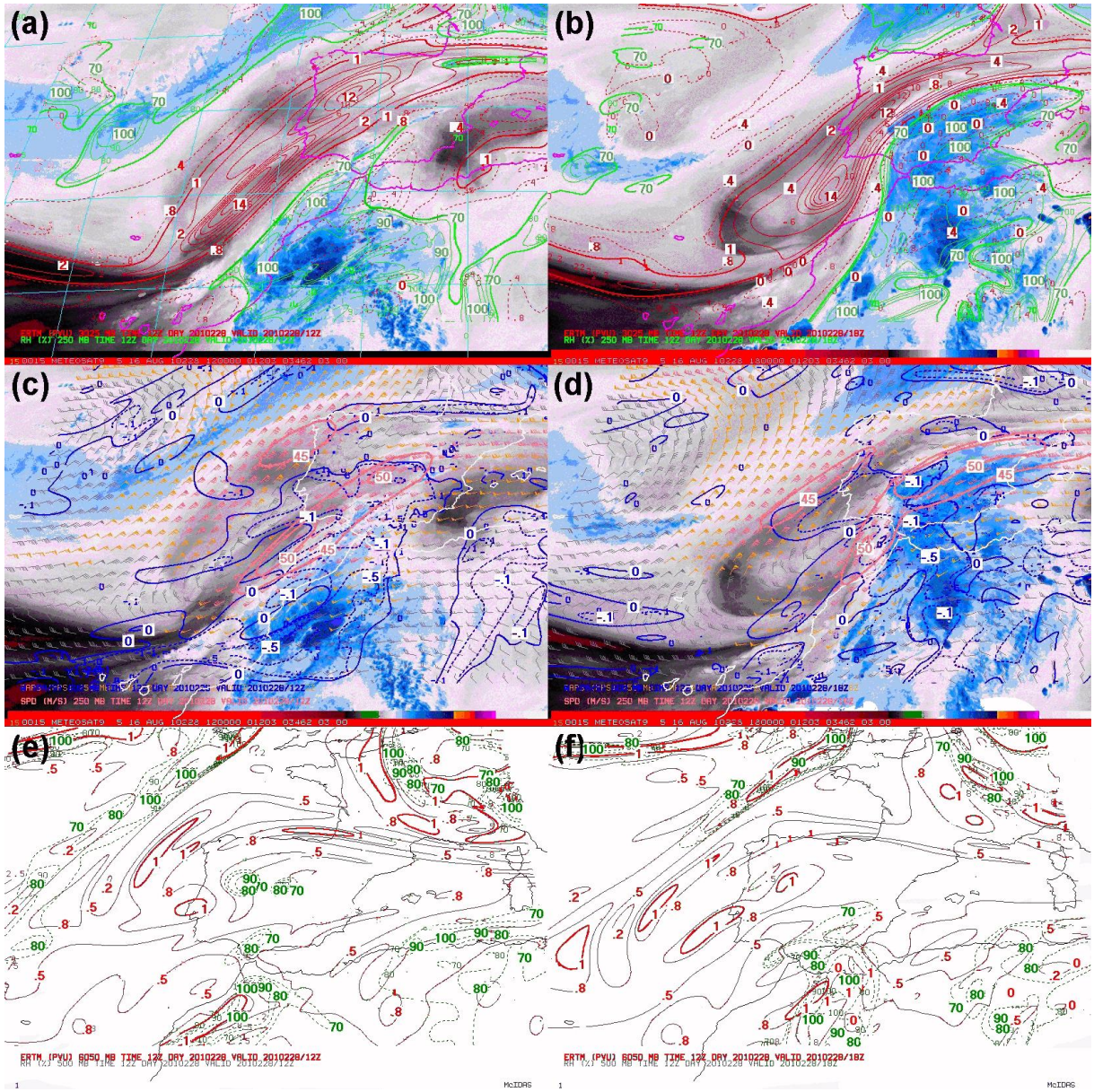

Figure 6. 16 August; Left column: 12:00 UTC images and analysis fields; right column: 18:00 UTC images and +06 forecasted fields. (a) and (b): WV 6.2 μm Meteosat images; PV (red; solid contours $\geq$ 1 PVU; dashed $<$ 1 PVU) and relative humidity (RH) at 250 hPa (green contours beginning 70%). (c) and (d): 6.2 μm Meteosat image, wind vectors (plotted as conventional wind barbs in knots) and isotachs at 250 hPa, and ω at 600 hPa (blue contours, dashed ascents). (e) and (f): PV at layer 600-500 hPa (solid contours; bold red contour: 1 PVU) and RH at 500 hPa (dashed green RH$>$70).

and upper-tropospheric jets in environments lacking large-scale saturation. They showed that simulated bands occurred in an environment with a nearly well-mixed, baroclinic boundary layer, positive convective available potential energy, and widespread negative PV. Individual bands initiated on the low-momentum side of vorticity banners downstream of mountains, and in association with frontogenetical ascent along baroclinic zones. In addition, they show that ascent caused by both frontogenesis and banded moist convection produced additional narrow regions of negative vorticity by transporting low momentum air upward and creating strong horizontal gradients in wind speed.

3.2 Lower level wind convergence

The field of mean sea level pressure (SLP) at 18:00 UTC (Figure 10) showed a low centred over the west of the Iberian Peninsula that was due to both the reflect of the trough at mid and upper levels, that was prolonged in a trough over the

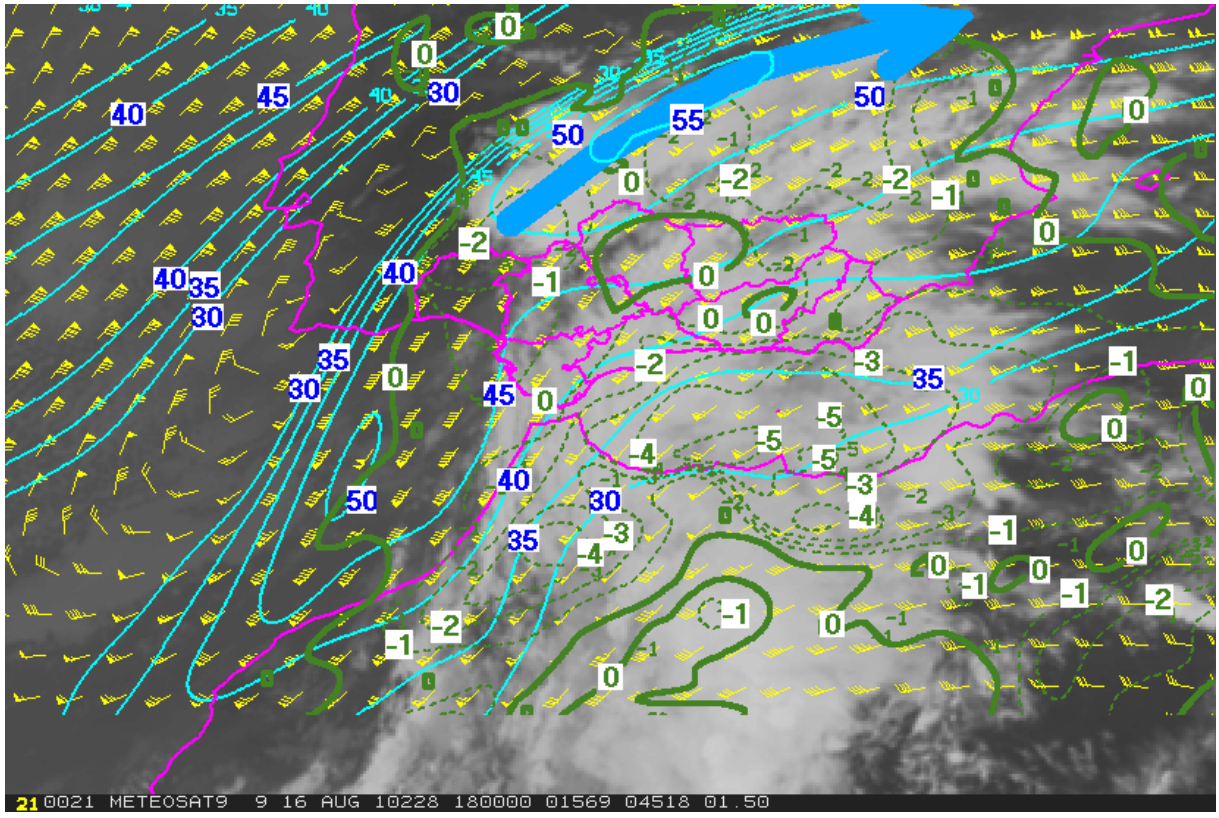

Figure 7. Wind vectors (plotted as conventional wind barbs in knots) and isotachs at 250 hPa (solid blue contours beginning in 30 m s^{-1}; interval: 5 m s^{-1}) and Lifted Index 700 (LI700) (dashed green contours for LI700<0; interval 1 K, and bold solid line for 0 K), all of them analysis fields, plotted over Meteosat IR 10.8 μm image at 18:00 UTC 16 August.

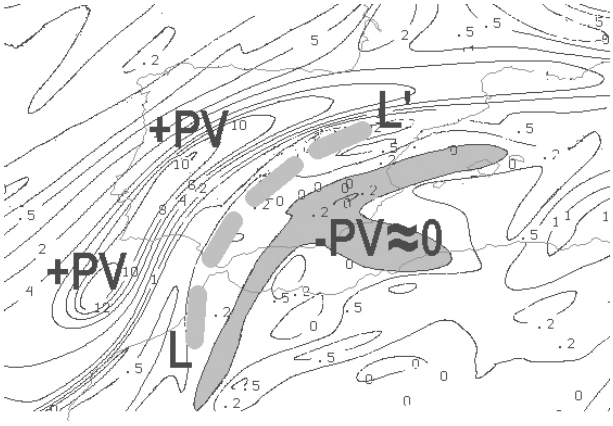

Figure 8. PV (PVU) at the layer 250-300 hPa at 18:00 UTC 16 August. Areas with PV $\sim$ 0 PVU are shaded grey.

eastern Atlantic, and to the thermal heating that generated a thermal low in the Peninsula in the warm season.

The SLP field is displayed with more detail in Figure 11a, where a stretched low along the middle and upper Guadalquivir Valley and westwards a mesoscale high are observed. This pressure distribution could have a thermal origin but it was also influenced by the upward and downward movements associated with the direct vertical circulation of the entrance zone of the upper level jet streak. As a result of the low pressure in the Guadalquivir valley, two low level airflows converged in the south of the Cordoba province. One of them was a relatively cool south-western flow coming from Atlantic and the other one was a warmer southerly flow coming from the Alboran Sea through the Guadalhorce gap, entering the valley and flowing perpendicular to the isotherms (Figure 11a) with characteristics of density current (all cited locations are indicated on Figure 1). The southern flow had a higher equivalent potential temperature (Figure 11b) than the south-western flow, establishing a significant air mass boundary in the convergence area that could have played a important role at the beginning of the event.

Figure 12 shows the maximum surface wind gusts in the ten minutes prior to 20:00 UTC measured in the AEMET automatic weather station network. The wind convergence in the area of Aguilar (bold red arrows) between the westerly flow along the Guadalquivir Valley, reflecting a wind relative maximum at low levels, and southerly flow through the Guadalhorce Gap, was maintained throughout the episode. The inset of Figure 12 shows the relatively low

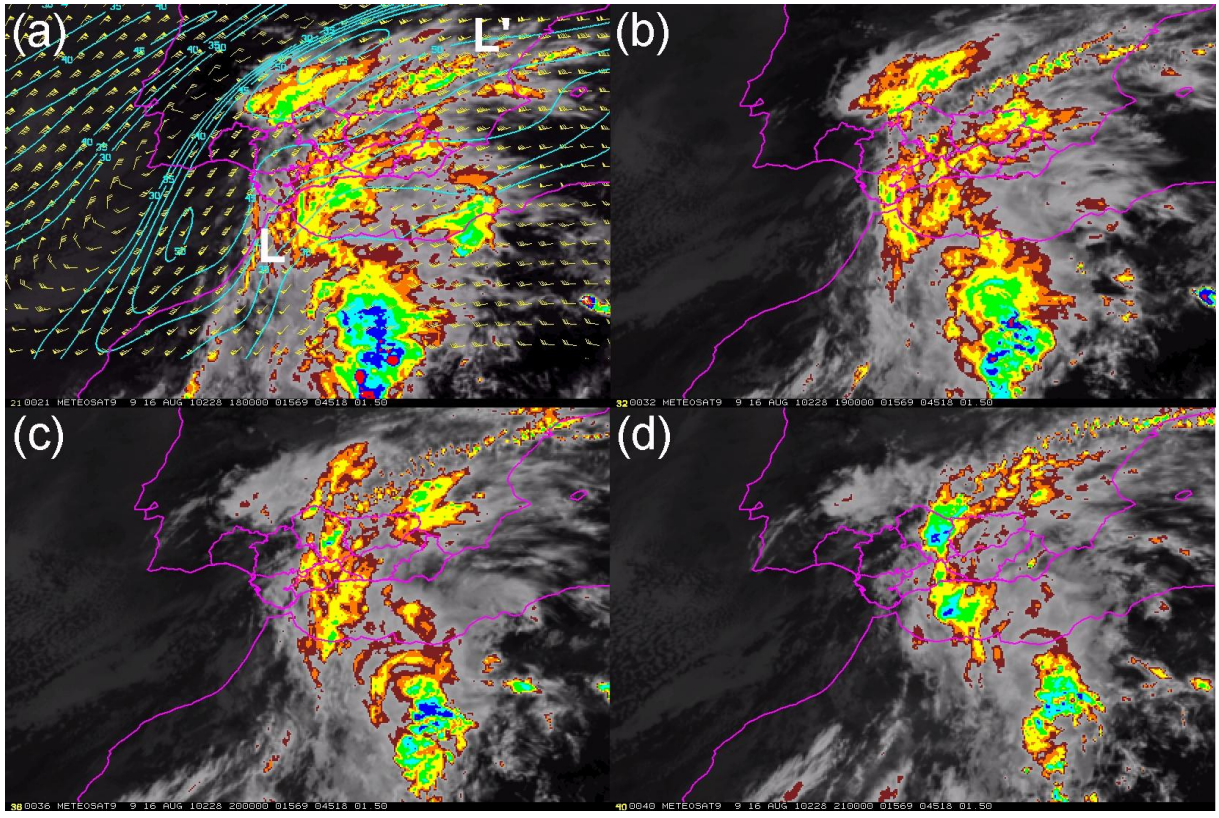

Figure 9. 10.8 μm IR images with the colder top clouds coloured at: (a) 18:00 UTC, with wind vectors (plotted as conventional wind barbs in knots) and isotachs at 250 hPa; (b) 19:00 UTC; (c) 20:00 UTC; and (d) 21:00 UTC on 16 August.

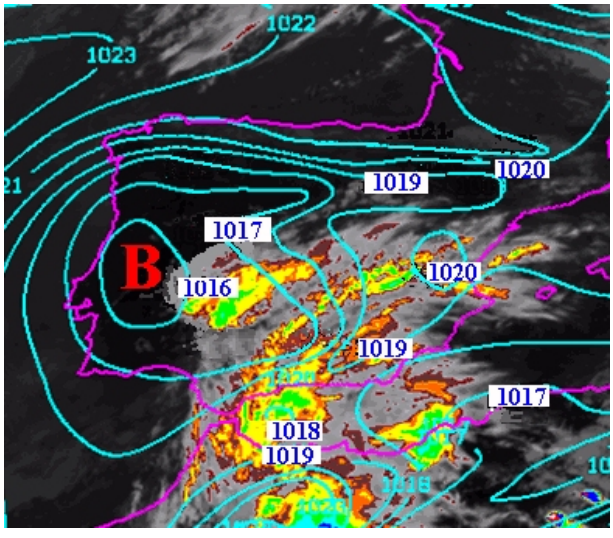

Figure 10. 18:00 UTC 16 August. Mean sea level pressure field (contour interval 1 hPa) plotted over IR-10.8 μm Meteosat-9 image.

temperature of the thunderstorm cold pool in Aguilar de la Frontera.

4 An interpretation of the persistence of the rainfall in Aguilar

As stated above, the presence of the line LL' of elevated convection (Figure 9) in the event was crucial. So a possible interpretation emerges from this evidence and from the analysis of the high and low level fields of the troposphere that is schematized in Figure 13.

A convergence area of different air masses existed in the south of the province of Cordoba at 18:00 UTC on 16 August. The first thunderstorm in Aguilar created a cold air pool in that area, the consequence of the evaporation of the falling precipitation (on surface and blue in Figure 13). The storm cold pool made positive horizontal vorticity (thick red arrow with plus). In addition, the vertical wind shear over the relative maximum westerly wind in low levels, along the Guadalquivir Valley, also made negative horizontal vorticity (thick red arrow with minus). Both these vorticities, associated with the cold pool and the low level westerly wind, interacted to create upward movements, represented in Figure 13a by a black arrow, which probably did not exceed the lifting condensation level (Figure 13a). Only the arrival over the

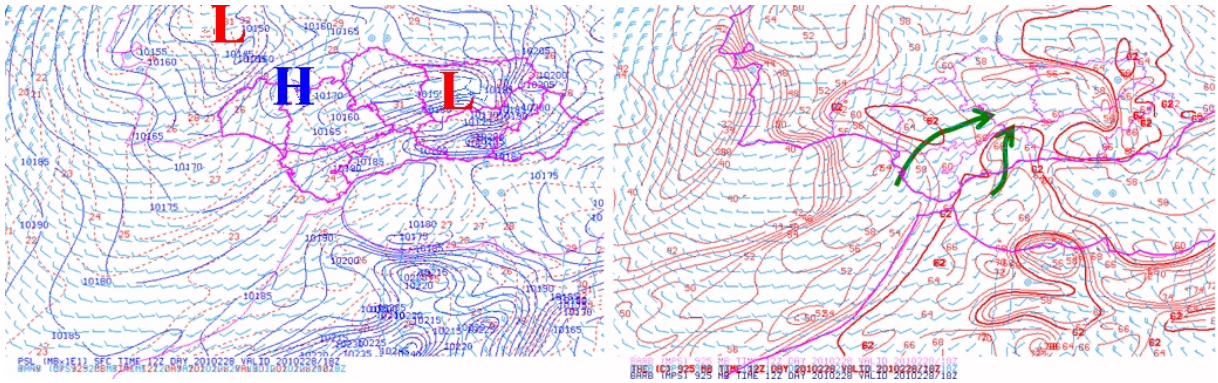

Figure 11. 18:00 UTC 16 August. (a, left) Wind vectors (plotted as conventional wind barbs in knots) and virtual potential temperature at 925 hPa (dashed red contours; interval: 1 K) and mean sea level pressure (solid blue contours; interval 0.5 hPa). (b, right) Wind vectors and equivalent potential temperature at 925 hPa (solid red contours; interval 2 K).

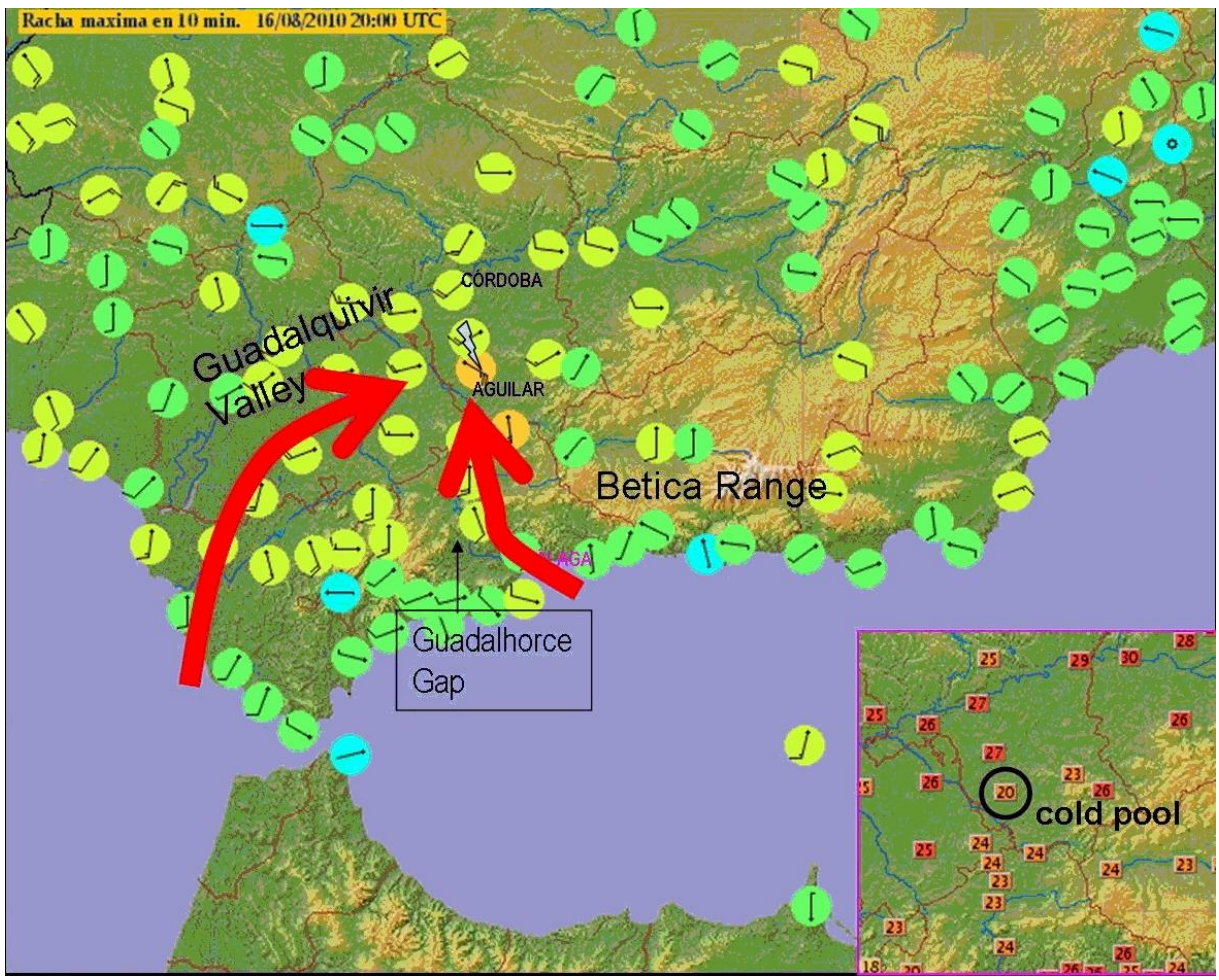

Figure 12. Map of maximum wind gusts vectors (plotted as conventional wind barbs in knots) at surface in ten minutes prior to 20:00 UTC from the AEMET automatic weather station network. The wind convergence on the area of Aguilar is schematized with bold arrows. The inset shows the relatively low temperature of the thunderstorm cold pool in Aguilar.

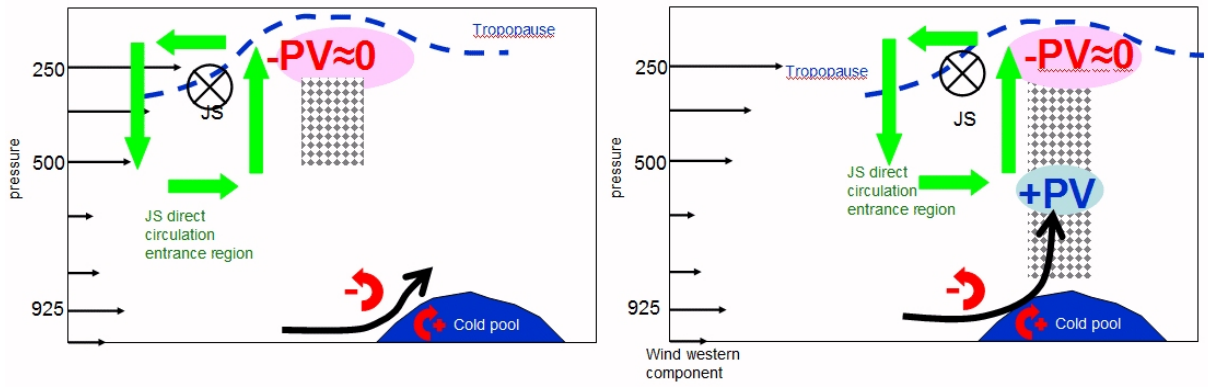

Figure 13. Schematic interpretation of the triggering of deep convection in the event. Actually the jet stream (JS) has a direction WSW-ENE and the direct circulation is not in the picture plane. Thin arrows along ordinate indicate the vertical profile of the western component of the environmental wind. Red arrows with plus or minus indicate sense of vorticity produced by the cold pool and by the environmental vertical wind shear.

convergence area of elevated convection cells organized in the line LL', associated with the ascents in the thermally direct vertical circulation in the entrance region of the jet streak (Figure 6), triggered the deep convection from lower levels (Figure 13b). This process lasted while the line LL' was sliding over the area. The wind speed and mid-level wind shear were weak, causing slow-moving storm cells and high precipitation efficiency.

5 Conclusions

An extraordinary heavy precipitation event exceeding 200 mm in 5 hours and causing significant flash flooding, occurred on 16 August 2010 in the town of Aguilar de la Frontera, in the south of Spain, an area with Mediterranean climate characterized by hot, dry summers, where the mean monthly precipitation for August is less than 10 mm. No other event of a similar magnitude affecting this region in the summer is known.

A tropical inverted trough, a mid-latitude positively tilted upper-trough over the eastern North Atlantic, and the mid-level African anticyclone interacted transporting tropical moisture towards subtropical West Africa forming an elongated tropical plume and a dry line at mid levels in the African north-western coast.

A mid-level frontogenesis and subsequently a weak cyclogenesis took place on the dry line that generated a deep-layer moistening and destabilization in the south of the Iberian Peninsula, and also caused the building of an outflow anticyclonic upper level jet.

A convergence of different air masses existed at low levels in the south of the province of Cordoba at 18:00 UTC on 16 August where a first thunderstorm created a cold air pool in Aguilar.

A band of elevated convection formed downstream of complex terrain of the western Betica Range, near the Strait of Gibraltar, within the ascending branch of the secondary circulation associated with the anticyclonic shear side of the entrance zone of the jet stream, where conditional, and possibly both, dry symmetric (negative PV), and inertial (negative absolute vorticity) instabilities were present.

The interaction between the ascents associated with the cells of the elevated convection band, crossing along over the area during the event, and the near surface ascent caused by the interaction between the relative maxima of winds at low level and the cold pool seem to have been determining in regenerating, once and again, the convection on Aguilar. The wind speeds through mid levels and vertical wind shears were weak, promoting slow-moving storms and increased precipitation efficiency.

On the synoptic scale, the location of the event, beneath the equatorward jet-entrance region of an upper-level jet streak, was similar to those documented for warm season heavy rain in the USA, and on a larger scale, the presence of moisture of tropical origin over the Iberian Peninsula, where intersected a region of forced ascent beneath the jet entrance region, made that the event was similar to PREs. However, while in PREs the tropical moisture is transported poleward from a TC, in the studied episode the tropical moisture was transported poleward directly from the convection of the African monsoon over the deep tropics of West Africa.

References

Augustine, J. A. and Caracena, F., 1994: *Lower-tropospheric precursors to nocutnral MCS development over the Central United States*, Wea Forecasting, **9**, 116–135.

Bosart, L. F. and Lackmann, G. M., 1995: *Postlandfall tropical cyclone reintensification in a weakly baroclinic environment: A case study of Hurricane David (September 1979)*, Mon Wea Rev, **123**, 3268–3291.

Brooks, H. E. and Stensrud, D. J., 2000: *Climatology of heavy rain events in the United States from hourly precipitation observa-*

tions, Mon Wea Rev, **128**, 1194–1201.

Browning, K. A., Thorpe, A. J., Montani, A., Parsons, D., Griffiths, M., Panagi, P., and Dicks, E. M., 2000: *Interactions of tropopause depressions with an ex-tropical cyclone and sensitivity of forecasts to analysis errors*, Mon Wea Rev, **128**, 2734–2755.

Caracena, F., Maddox, R. A., Hoxit, L. R., and Chappell, C. F., 1979: *Mesoanalysis of the Big Thompson storm*, Mon Wea Rev, **107**, 1–17.

Cote, M. R., 2007: Predecessor rain events in advance of tropical cyclones, M.S. thesis, Department of Atmospheric and Environmental Sciences, University at Albany, State University of New York, 200 pp., Available online at http://cstar.cestm.albany.edu/CAP_Projects/Project10/index.htm.

Doswell III, C. A., Brooks, H. E., and Maddox, R. A., 1996: *Flash flood forecasting: An ingredients-based methodology*, Wea Forecast, **11**, 560–581.

Font, I., 1983: Climatología de España y Portugal, Instituto Nacional de Meteorología, Madrid, 296 pp.

Galarneau, T. J., Bosart, L. F., and Schumacher, R. S., 2010: *Predecessor rain events ahead of tropical cyclones*, Mon Wea Rev, **138**, 3272–3297.

Garía-Dana, F., Font, R., and Rivera, A., 1982: Situación meteorológica durante el episodio de lluvia intensa en el levante español durante octubre de 1982, Instituto Nacional de Meteorología, Apartado 285, E-28071 Madrid, Spain, 68 pp.

Glass, F. H., Ferry, D. L., Moore, J. T., and Nolan, S. M., 1995: Characteristics of Heavy Convective Rainfall Events Across the Mid-Mississippi Valley During the Warm Season: Meteorological Conditions and a Conceptual Model, Preprints, 14th Conf. on Wea. Analysis and Forecasting, Dallas, TX, 34-41.

Junker, N. W., Schneider, R. S., and Fauver, S. L., 1999: *A study of heavy rainfall events during the Great Midwest Flood of 1993*, Wea Forecast, **14**, 701–712.

Maddox, R. A., Hoxit, L. R., Chappell, C. F., and Caracena, F., 1978: *Comparison of Meteorological Aspects of the Big Thompson and Rapid City Flash Floods*, Mon Wea Rev, **106**, 375–389.

Maddox, R. A., Chappell, C. F., and Hoxit, L. R., 1979: *Synoptic and meso-α-scale aspects of flash flood events*, Bull Amer Meteor Soc, **60**, 115–123.

Martinez, C., Campins, J., Jansà, A., and Genovés, A., 2008: *Heavy rain events in the Mediterranean : an atmospheric pattern classification*, Adv Sci Res, **2**, 61–64.

Miller, M., Buizza, R., Haseler, J., Hortal, M., Janssen, P., and Untch, A., 2010: Increased resolution in the ECMWF deterministic and ensemble prediction systems, ECMWF Newsletter No. 124.

Moore, J. T., Glass, F. H., Graves, C. E., Rochette, S. M., and Singer, M. J., 2003: *The environment of warm-season elevated thunderstorms associated with heavy rainfall over the central United States*, Wea Forecast, **18**, 861–878.

Pontrelli, M. D., Bryan, G., and Fritsch, J. M., 1999: *The Madison County, Virginia, flash flood of 27 June 1995*, Wea Forecast, **14**, 384–404.

Romero, R., Sumner, G., Ramis, C., and Genovés, A., 1999: *A classification of the atmospheric circulation patterns producing significant daily rainfall in the Spanish Mediterranean area*, Int J Climatol, **19**, 765–785.

Schumacher, R. S. and Johnson, R. H., 2005: *Organization and environmental properties of extreme-rain-producing mesoscale convective systems*, Mon Wea Rev, **133**, 961–976.

Schumacher, R. S. and Johnson, R. H., 2006: *Characteristics of U.S. extreme rain events during 1999-2003*, Wea Forecast, **21**, 69–85.

Schumacher, R. S., Schultz, D. M., and Knox, J. A., 2010: *Convective snowbands downstream of the rocky mountains in an environment with conditional, dry symmetric, and inertial instabilities*, Mon Wea Rev, **138**, 4416–4438.

Simmons, A. J., Burridge, D. M., Jarraud, M., Girard, C., and Wergen, W., 1989: *The ECMWF medium-range prediction model: Development of the numerical formulations and the impact of increased resolution*, Meteorol Atmos Phys, **40**, 28–60.

Trier, S. B., Davis, C. A., Ahijevych, D. A., Weisman, M. L., and Bryan, G. H., 1996: *Mechanisms Supporting Long-Lived Episodes of Propagating Nocturnal Convection within a 7-Day WRF Model Simulation*, J Atmos Sci, **63**, 2437–2461.

Uccellini, L. W. and Johnson, D. R., 1979: *The coupling of upper and lower tropospheric jet streaks and implications for the development of severe convective storms*, Mon Wea Rev, **107**, 682–703.